# Products and Mechanism of the Thermal Cross-Linking of Benzocyclobutene-Terminated Bisphenol A Polycarbonates

**M. J. Marks,* J. S. Erskine, and D. A. McCrery**

*Texas Polymer Center, Dow Chemical U.S.A., Freeport, Texas 77541*

*Received March 16, 1994; Revised Manuscript Received May 11, 1994*•

ABSTRACT: Hydrolysis of cross-linked benzocyclobutene-terminated Bisphenol A polycarbonate (BCB PC) gave a mixture of phenolic compounds which were shown by liquid chromatography/mass spectroscopy to consist of Bisphenol A (BA) and related compounds, unreacted 4-hydroxybenzocyclobutene, hydroxy-substituted stilbenes and/or dibenzocyclooctadienes, and hydroxy-substituted tetrahydronaphthalenes. None of the observed BCB cross-linking products result from reaction of the BCB group with the BA PC chain. Also, no high molecular weight BCB derivatives were found. The same products were found in the hydrolysate of cross-linked bis(benzocyclobutenyl) carbonate. The selectivity of BCB homopolymerization appears inconsistent with a radical chain reaction mechanism but can be explained by a series of pericyclic reactions involving Diels–Alder cycloadditions, retro-ene reactions, and sigmatropic rearrangements.

## Introduction

Benzocyclobutene-terminated bisphenol A polycarbonates (BCB PC's, 1) are a new class of thermally cross-

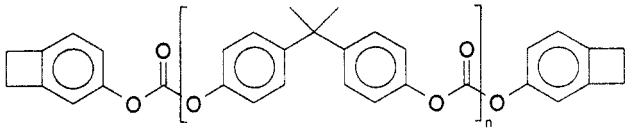

1

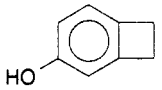

2

linkable engineering thermoplastics.[1-3] Linear BCB PC's derived from 4-hydroxybenzocyclobutene (BCB-OH, 2) can be prepared by interfacial polycondensation of Bisphenol A (BA), BCB-OH, and phosgene to form polymers having molecular weights controlled by the relative amounts of BCB-OH and BA employed. Cross-linking of these polymers at about 200–300 °C occurs by an exothermic process at rates dependent on temperature. The properties of these new thermosets depend generally on their cross-link density. Low cross-link density BCB PC's are relatively tough and have good solvent and ignition resistance, yet thermally process like thermoplastics before cross-linking. High cross-link density BCB PC's behave more like high-performance thermosets[4] and have relatively high fracture toughness.

Although considerable research on BCB-based thermosets has been conducted in the last several years,[5] the products formed by BCB homopolymerization have not been previously identified. Previous work has shown that BCB undergoes a thermally allowed ring-opening isomerization to *o*-quinodimethane (Scheme 1).[6] It has been proposed that BCB homopolymerization proceeds by the Diels–Alder cycloaddition of two *o*-quinodimethanes to form a "spirodimer" which in turn fragments into a diradical that couples to form poly(*o*-xylene) and dibenzocyclooctane.[7,8] Alternatively, the use of BCB compounds

**Scheme 1. Known and Previously Proposed BCB Reactions**

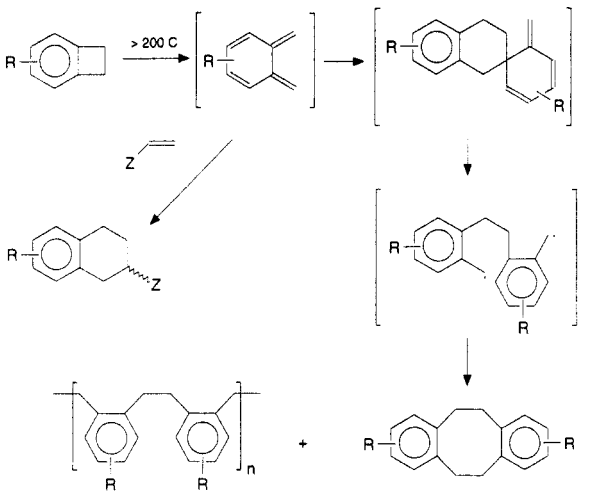


as latent dienes in Diels–Alder cycloadditions with dienophiles has been exploited in organic synthesis for many years (Scheme 1),[9-11] and the reaction of BCB moieties with internally bonded olefins to prepare high cross-link density thermosets has been recently studied.[12,13]

In this study cross-linked BCB PC's were hydrolyzed to produce mixtures of BA and poly-BCB-OH products. These mixtures were separated using reversed-phase liquid chromatography, and the components were identified by mass spectroscopy (LC/MS), providing the first direct analysis of BCB homopolymerization products. To account for the selectivity of the products observed, a pericyclic reaction mechanism is proposed as an alternative to the previously proposed radical process.

## Experimental Section

**Chemicals.** Dichloromethane (Dow Chemical, technical grade), 50 wt % aqueous sodium hydroxide (Fisher Scientific), potassium hydroxide (Fisher Scientific), methanol (Fisher Scientific), absolute ethanol (Fisher Scientific), triethylamine (TEA; Aldrich Chemical Co.), tetrahydrofuran (THF; Fisher Scientific), and phosgene (5-lb. cylinders from Matheson Gas Products) were used as received. BCB PC ($M_n$ = 4500)[1] and 4-hydroxybenzocyclobutene[32] (BCB-OH) were prepared as previously described.

**Hydrolysis of Cross-Linked BCB PC.** A mixture of 1 g of cross-linked BCB PC, 9 g of THF, and 5 g of 20 wt % KOH in methanol was shaken in a capped vial for 18 h at room temperature. A 0.5-mL aliquot of the supernatent solution was

* Author to whom correspondence should be addressed.

• Abstract published in *Advance ACS Abstracts*, June 15, 1994.

0024-9297/94/2227-4114$04.50/0 

**Scheme 2. Hydrolysis of BCB PC**

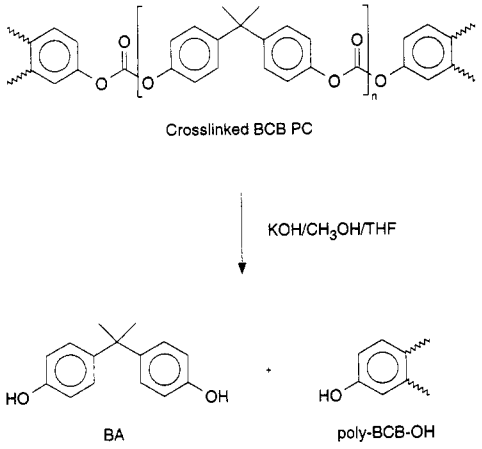


diluted with 10 mL of THF, acidified with 2 drops of concentrated HCl, and then filtered for LC analysis.

**Analytical Methods.** LC analysis was done on a Hewlett-Packard (HP) Model 1090 system connected to a UV diode-array detector and fitted with a Scientific Glass Engineering glass-lined column (150 × 4 mm) containing Spherisorb ODS2 (3 μm). A mobile phase gradient of 20% THF/80% water at 0 min, 30% THF at 10 min, 60% THF at 30 min, 50% THF at 50 min, and 100% THF at 50 min was used at a flow rate of 0.5 mL/min. The LC/MS analyses were conducted using the above LC interfaced to a Finnigan SSQ-710 quadrupole mass spectrometer. The mobile phase gradient at 0.3 mL/min was as follows: 20% THF/80% water at 0 min, 30% THF at 10 min, 30% THF at 20 min, 40% THF at 40 min, and 80% THF at 90 min. The LC was coupled to the mass spectrometer by a either a polyimide belt or a Finnigan particle beam interface. In the former (for BCB PC) the vaporizor and cleanup heaters were set at 270 °C, and in the latter (for bis-BCB $CO_3$) the supplied helium gas pressure was set to provide a nebulizer flow of approximately 0.7 standard liters per minute (SLPM) with the interface desolvation chamber temperature set to 60 °C.

Mass spectra were obtained on eluted components using conventional electron impact (EI) ionization techniques. The mass spectrometer source temperature was set to 250 °C, and mass spectra were collected in the mass range from 75 to 650 amu at 2-s intervals.

**Synthesis of Bis(benzocyclobutenyl) Carbonate (15).** To an 8-oz. jar were added 0.5 g of BCB-OH, 3 g of $CH_2Cl_2$, 10 g of water, and 0.35 g of 50% aqueous NaOH. The mixture was stirred magnetically to dissolve the BCB-OH. Then 4.6 mL of a 8.2 wt % solution of phosgene in $CH_2Cl_2$ was added with stirring. A few drops of aqueous NaOH were added to increase the pH of the aqueous phase to 12–13, and then 1 drop of TEA was added and the mixture was stirred for 5 min. The aqueous phase was removed, and the organic phase was washed once with 1 N HCl and four times with water. The organic phase was dried with sodium sulfate and evaporated to yield 0.47 g (85%) of a pale yellow solid (mp = 127 °C). Recrystallization from ethanol gave white crystals. Anal. Calcd for $C_{17}H_{14}O_3$: C, 76.6; H, 5.3. Found: C, 76.05 ± 0.08; H, 5.14 ± 0.17.

## Results and Discussion

Linear BCB PC's were prepared by interfacial polycondensation of BCB-OH, BA, and phosgene and were subsequently cross-linked by compression molding at 200–300 °C.[1,2] The resulting networks were hydrolyzed in KOH/methanol/THF at room temperature to yield a mixture of phenolic compounds consisting of BA and the previously undefined poly-BCB-OH (Scheme 2). The cross-linked BCB PC's swell in the reaction medium, and as the hydrolysis proceeds the gels break down. Prior to LC analysis the samples were acidified with aqueous HCl to convert the potassium phenoxides into phenolics.

**LC/MS Analysis of Bisphenol A.** The commercial-grade BA used to prepare BCB PC's contains small amounts of phenols other than *p,p'*-BA. The LC of BA (Figure 1) shows five major components, the first and largest of which is *p,p'*-BA (LC peak 1). The MS of peak 2 (Figure 2) shows a molecular ion ($M^+$, *m/e* 228) and fragmentation pattern corresponding to *o,p'*-BA[14] (3). The

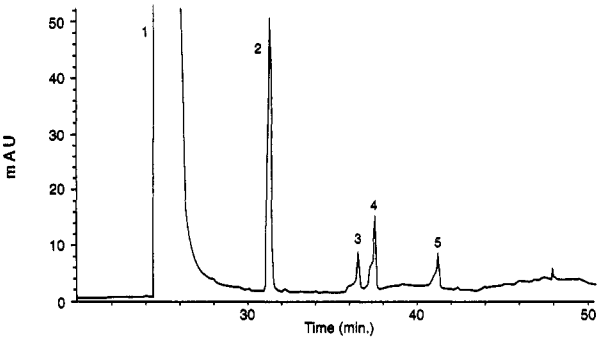


**Figure 1.** LC of Bisphenol A (BA).

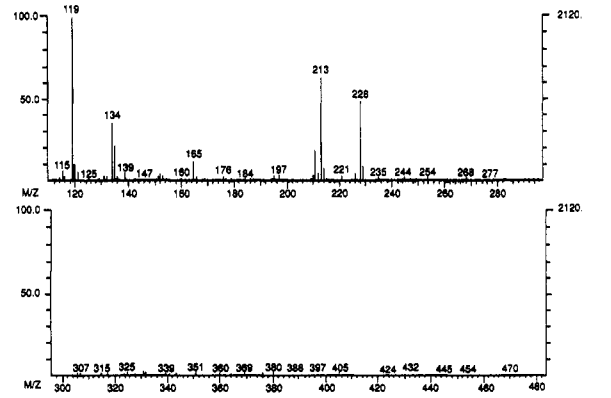


**Figure 2.** MS of peak 2 in LC of BA (*o,p'*-BA).

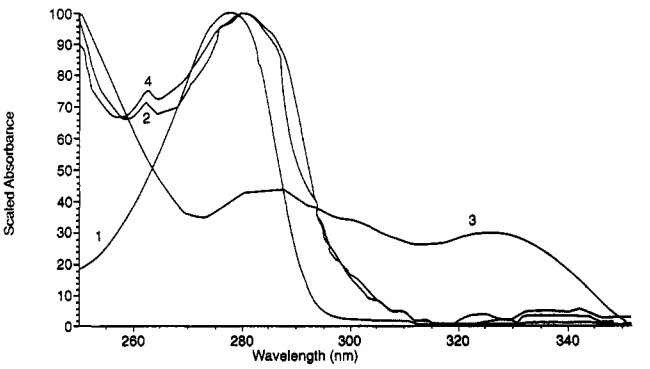


**Figure 3.** UV spectra of peaks 1–4 in LC of BA.

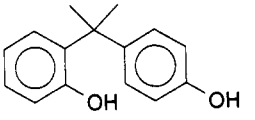


3

UV spectra of the other three peaks indicate phenolic and/or extended conjugated structures (Figure 3). MS data could not be obtained on the other three components due to their low concentration in the sample. However, the concentrations of these compounds greatly increases upon heating BA to 250 °C under nitrogen. LC/MS analysis of a heated BA sample gave adequate concentrations of the latter three compounds and showed that peak 3 has a $M^+$ at *m/e* 320 (Figure 4) and peaks 4 and 5 both have $M^+$ at *m/e* 454 (Figures 5 and 6).

The mass spectrum of peak 3 shows a $M^+$ at *m/e* 320 (Figure 4) and indicates this compound to be (4-hydrox-

yphenyl)-Bisphenol A (4; 2-position isomer shown in Scheme 3) or its phenoxy isomer. The major fragmentation pathway of this compound occurs by loss of a methyl radical (M-15) to *m/e* 305 and lesser amounts of fragmentation products by loss of a hydroxyphenyl (or phenoxy) radical (M-93) to *m/e* 227 and a subsequent loss of a methyl radical (M-108) at *m/e* 211, all consistent with the proposed structure. (Fragmentation is shown stepwise for clarity; all observed cationic fragments without the neutral species and generally only the most stable carbon-centered cation are depicted.) The fragmentation patterns observed do not distinguish between the possible triphenol and diphenolic ether isomers.

The mass spectra of peaks 4 and 5 (Figures 6 and 7, respectively) in the LC of BA both show a $M^+$ at *m/e* 454 and indicate these compounds to be (4-hydroxyphenyl)-trisphenols (5 and/or 6,only one isomer of each shown) or

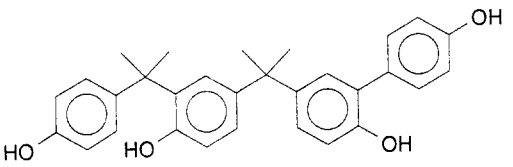


5

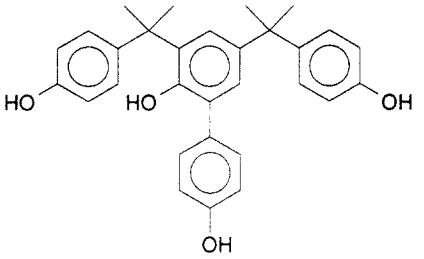


6

its phenoxy isomers. The major fragmentation pathway of these compounds involves methyl radical losses (M-15) to *m/e* 439 (Scheme 4). The loss of methyl and water radicals (to *m/e* 421) is similar to the fragmentation of *o,p'*- and *o,o'*-BA[15] which lose *o*-hydroxy groups. Loss of hydroxyphenyl and hydrogen radicals (M-94) to *m/e* 360 and subsequent loss of a methyl radical (M-109) to *m/e* 345 are similar fragmentations as seen in compound 4. The loss of allene (M-149) from *m/e* 345 radical gives the *m/e* 305 ion. Again the fragmentations observed do not distinguish between the several possible isomers.

Compounds 4–6 could arise from substitution of hydroxyphenyl or phenoxy radicals on *p,p'*-BA for the former and on trisphenol 7 for the latter two. A purely statistical

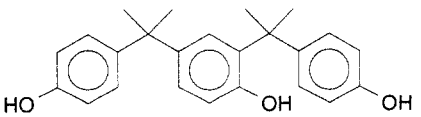


7

reaction such as this with 7 would give a 2:1 mixture of compounds 8 and 9, the same as the relative area percentages of peaks 4 and 5 in the LC.

**LC/MS Analysis of BCB PC Hydrolysate.** The LC of cross-linked BCB PC hydrolysate (Figure 7) shows the appearance of several new compounds which arise from BCB reactions. Of the 21 peaks in this chromatograph, 16 are due to new products formed during BCB PC cross-linking. As explained below, these products result solely from BCB homopolymerization, and their assigned structures are summarized in Table 1, with their relative area

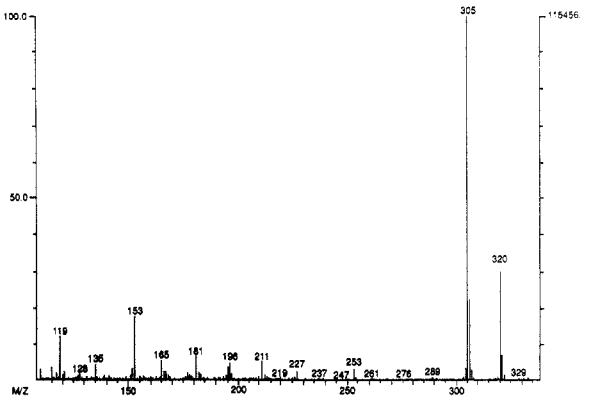

**Figure 4.** MS of peak 3 in LC of BA.

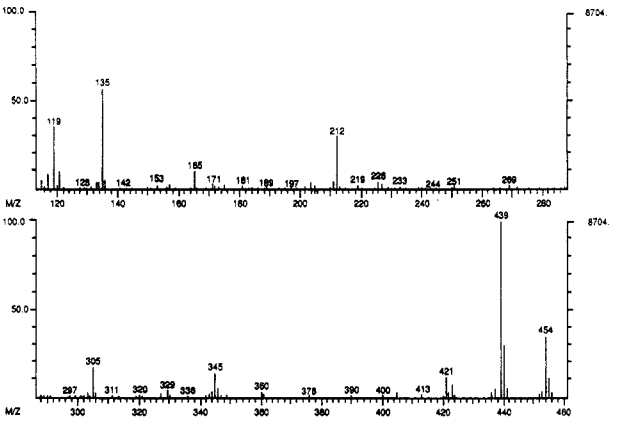

**Figure 5.** MS of peak 4 in LC of BA.

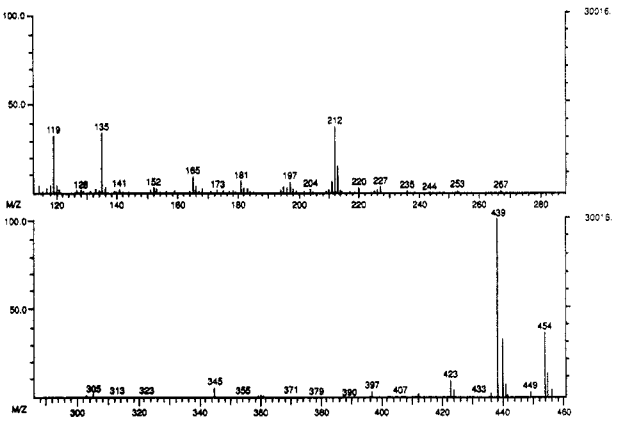

**Figure 6.** MS of peak 5 in LC of BA.

percent (excluding BA components) appearing in Table 2. Peak 1 in this LC is BCB-OH (2) as shown by comparison to an authentic sample. Not found in this LC is 3,4-dimethylphenol (8), which could form from addition of two hydrogen atoms to BCB-OH.

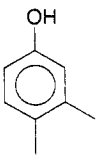


8

The UV spectra of several of the larger latter peaks show absorbance maxima near 280 nm, indicating phenolic or extended conjugated structures (Figure 8). Peaks 2–21 in the LC were analyzed by LC/MS. The mass spectra of peaks 2 and 3 are essentially identical and show $M^+$ at *m/e*

**Scheme 3. MS Fragmentation of (2-Hydroxyphenyl)-Bisphenol A (4)**

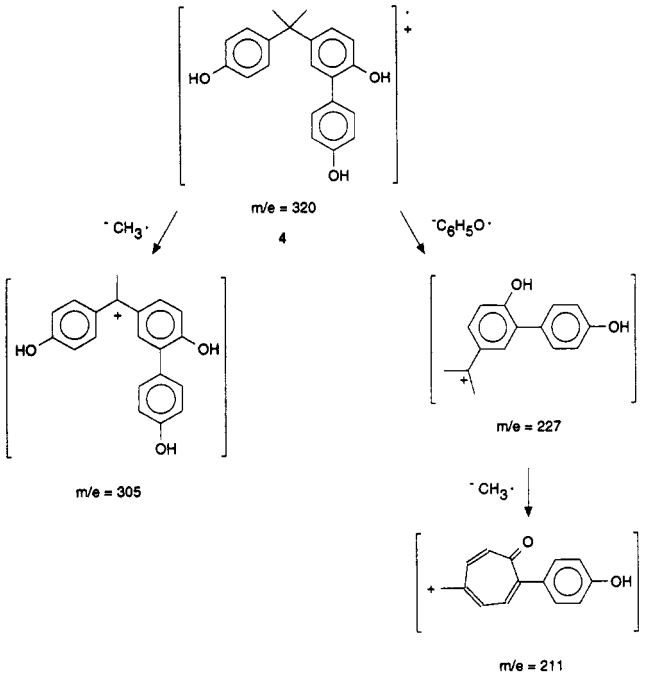


**Scheme 4. MS Fragmentation of (2-Hydroxyphenyl)-trisphenol (5)**

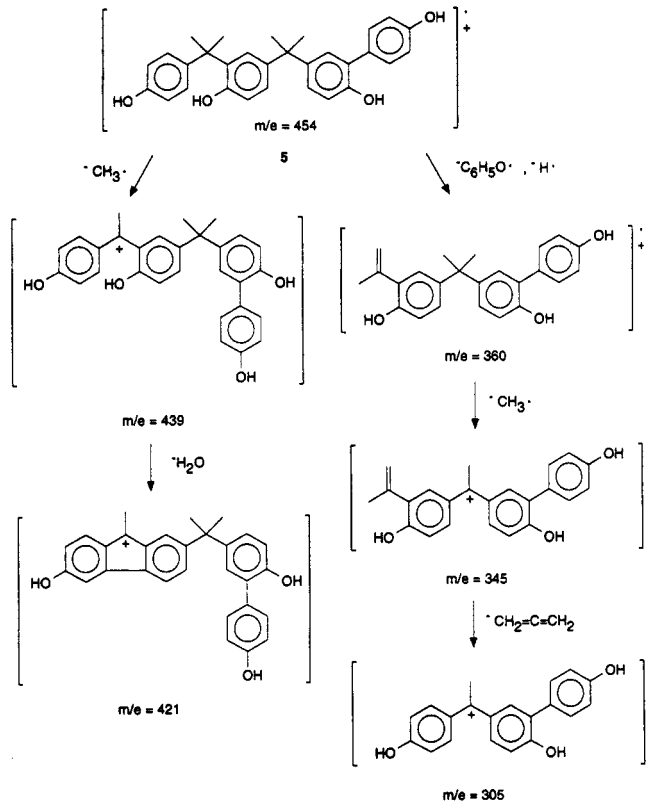


240 (Figures 9 and 10, respectively). Both dihydroxydimethylstilbene (**9**; six total isomers possible, three *cis* and three *trans*) and dihydroxydibenzocyclooctadiene (**10**; two isomers possible) are consistent with the observed fragmentation patterns of these two peaks. It would be reasonable to find the several isomers of **9** only partially resolved, perhaps grouped as the two types of geometric isomers. The major ion fragments observed result from three paths: (a) ionization followed by homolysis to BCB-OH (**2**); (b) homolysis of the phenyl–$sp^2$ carbon bond; and (c) loss of methyl radical, cyclization to a dihydroanthracene derivative, and another methyl radical loss to dihydroxyanthracene (Scheme 5). The mass spectra of the hydrocarbon analogs of compounds **9** and **10** (2,2′-dimethylstilbene[16] and dibenzocyclooctadiene[17]) show almost identical fragmentation patterns, with major ions

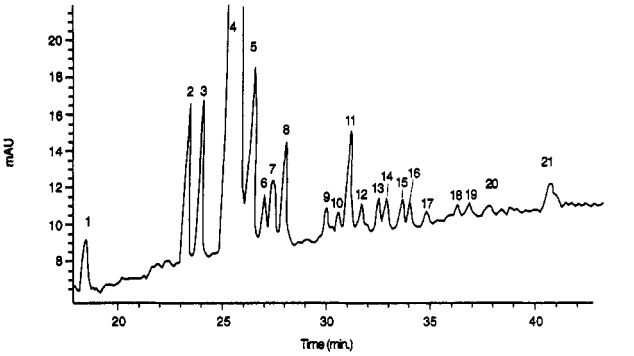


**Figure 7.** LC of cross-linked BCB PC hydrolysate.

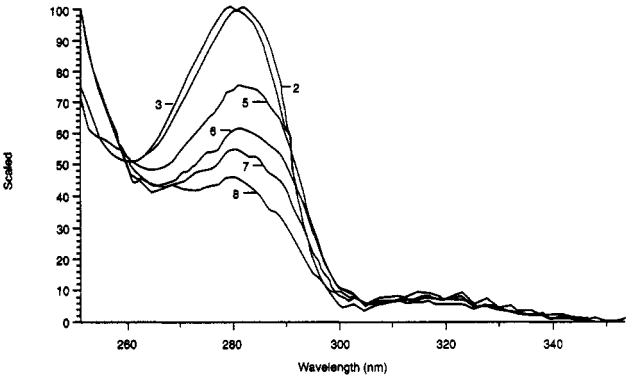


**Figure 8.** UV spectra of selected peaks in LC of cross-linked BCB PC hydrolysate.

**Table 1. Poly-BCB-OH Compounds in Cross-Linked BCB PC and Bis-BCB $CO_3$ Hydrolysates**

| LC peak no. | structure | MW |
|---|---|---|
| 1 | 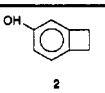 2 | 120 |
| 2, 3 | 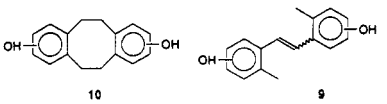 10 9 | 240 |
| 5–8 | 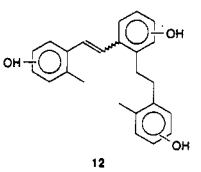 12 | 360 |
| 9, 10, 12–16 | 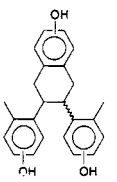 13 | 360 |
| 17–19 | 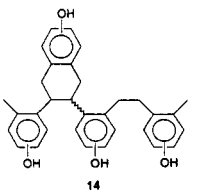 14 | 480 |

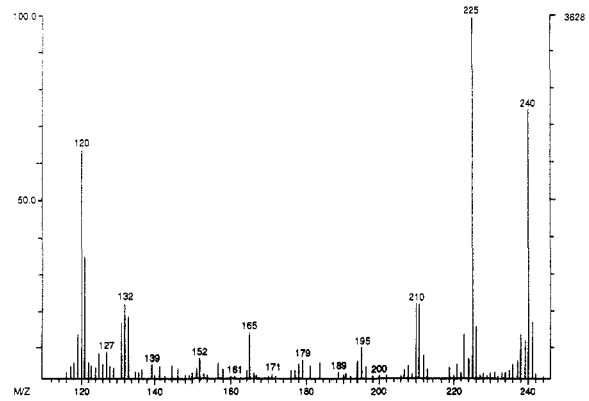

**Figure 9.** MS of peak 2 in LC of cross-linked BCB PC hydrolysate.

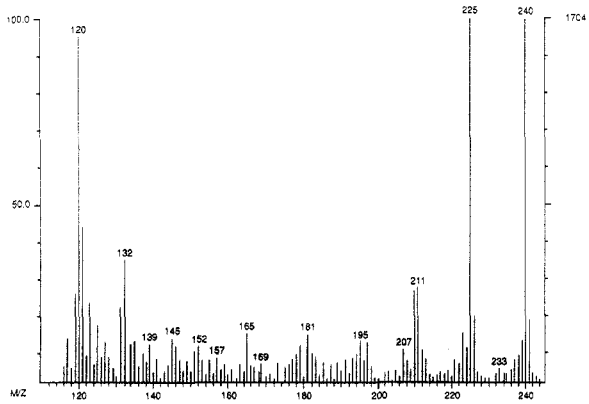

**Figure 10.** MS of peak 3 in LC of cross-linked BCB PC hydrolysate.

analogous to those listed above. The only significant difference in the MS's of these two hydrocarbons is the appearance of a large M-108 (BCB) ion in dibenzocyclooctadiene which is only a minor fragment in 2,2'-dimethylstilbene. Peaks 3 and 4 both show large M-120 (BCB-OH) ions, but since stilbene compounds are known to completely scramble before fragmentation,[18] this difference alone is not considered enough to distinguish between the two possibilities for either peak. Dibenzocyclooctadiene could isomerize to the stilbene before fragmentation by homolytic cleavage to a ditolyl radical followed by intramolecular hydrogen atom abstraction. Another isomer which would also have a very similar mass spectrum[19] is the BCB-OH spirodimer 11, formed by the

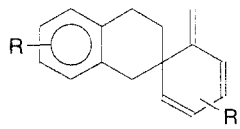

11

cycloaddition of two ring-opened BCB's, but, since the hydrocarbon analog is known to be thermally unstable,[19] this dimer would not survive the cross-linking conditions experienced by this sample.

Selected ion chromatograph (SIC) plots of *m/e* 240 and 225 along with the recontructed ion chromatograph (RIC), which shows the total ion current incident on the detector (Figure 11), show that peaks 3 and 4 in the LC are the only compounds present in the mixture having significant ions at *m/e* 240.

Peaks 4, 11, 20, and 21 in the LC of the cross-linked BCB PC hydrolysate are *p,p'*-BA, *o,p'*-BA, and phenols **5** and **6**, respectively, as seen in BA and described above.

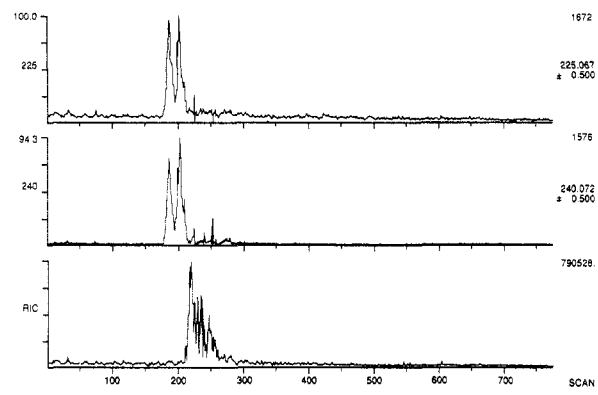

**Figure 11.** SIC's of *m/e* 225 and 240 in LC of cross-linked BCB PC hydrolysate.

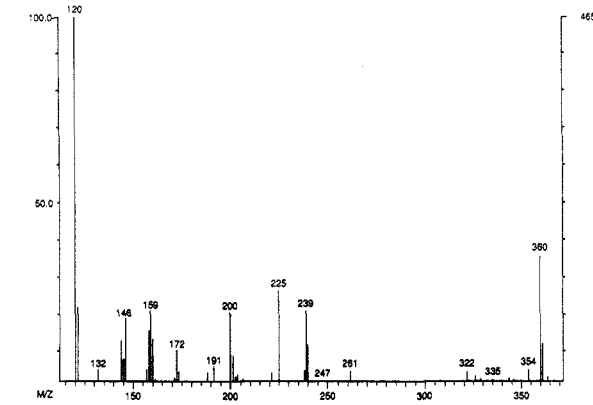

**Figure 12.** MS of peak 5 in LC of cross-linked BCB PC hydrolysate.

**Table 2. Relative LC Area Percent of Poly-BCB Products**

| 0.10 m/m BCB PC (Figure 7) | | bis-BCB $CO_3$ (Figure 16) | |
|---|---|---|---|
| LC peak no. | area % | LC peak no. | area % |
| 1 | 5.44 | 1 | 5.60 |
| 2 | 13.80 | 2 | 18.65 |
| 3 | 13.87 | 3 | 19.69 |
| 5 | 18.15 | 4 | 8.88 |
| 6 | 3.86 | 5 | 23.09 |
| 7 | 7.63 | 6 | 5.05 |
| 8 | 9.70 | 7 | 9.17 |
| 9 | 4.75 | 8 | 9.86 |
| 10 | 2.53 | | |
| 12 | 4.30 | | |
| 13 | 3.31 | | |
| 14 | 3.52 | | |
| 15 | 3.16 | | |
| 16 | 2.38 | | |
| 17 | 1.20 | | |
| 18 | 1.20 | | |
| 19 | 1.20 | | |

The MS of peak 5 shows a $M^+$ at *m/e* 360 and a fragmentation pattern consistent with a dehydrotris(hydroxyxylene) (**12**; Figure 12). These major fragments can be accounted for by four paths: (a) homolysis of the disubstituted ethane carbon–carbon bond to a stilbenic ion and dimethylphenol ion, which subsequently loses a hydrogen atom to give BCB-OH; (b) cleavage of the middle phenyl ring into two and four carbon chain fragments to form, after respective cyclizations, hydroxymethylnaphthalene and dihydroxymethyldihydrobiphenyl, which subsequently loses two hydrogen atoms to the substituted biphenyl ion; (c) cleavage of the phenyl ring in half to form, after respective cyclizations, dimethylhydroxynaphthalene and a (hydroxytolyl)cyclopentenone; and (d) homolysis of the phenyl–ethane $sp^3$ carbon bond to yield stilbenic and ethylhydroxytolyl ions (Scheme 6). The mass

**Scheme 5. MS Fragmentation of BCB-OH Dimer 9**

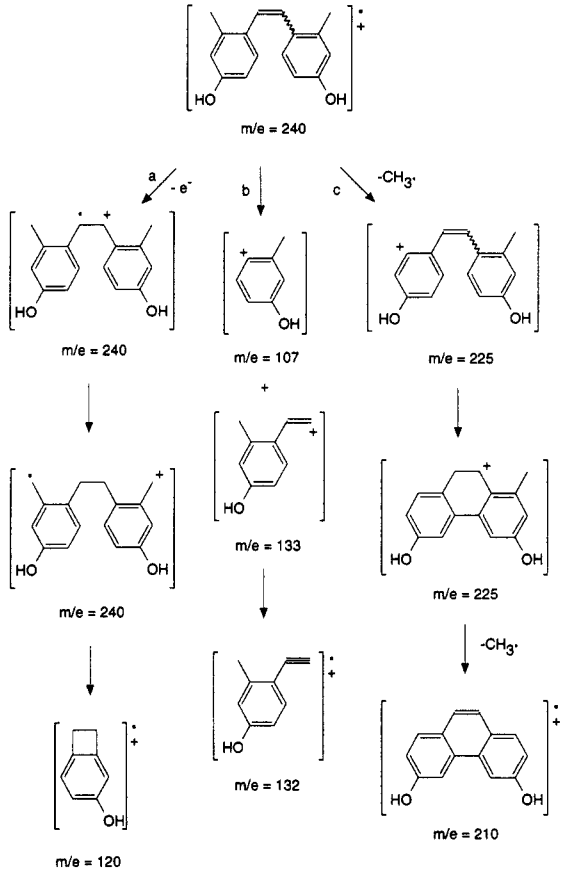


spectra of peaks 6–8 show similar results. The hydroxy substitution in structure **12** results in the possibility of eight *cis* and eight *trans* regioisomers, and it is not surprising that all of them are not resolved by the LC method.

The MS of peak 9 also shows a $M^+$ at *m/e* 360, but the fragmentation pattern is consistent with isomers of 2,3-bis(hydroxytolyl)hydroxy-1,2,3,4-tetrahydronaphthalene (**13**) rather than **12** (Figure 13). This peak shows significant ions for M-2, M-3, M-4, M-108, and M-240 which correspond to losses of 2, 3, and 4 hydrogen atoms to *m/e* 358, 357, and 356, loss of hydroxytolyl and hydrogen radicals to *m/e* 252, and formation of BCB-OH for the *m/e* 120 ion (Scheme 7). The hydrogen losses lead to aromatization of the unsaturated ring, and the intensities of these losses seen are similar to those found in the MS of tetrahydronaphthalene.[20] The dissociation of the hydroxytolyl radical leads to a stable dihydronaphthalene derivative. Neither of these two types of fragmentations is observed in the previous 360 $M^+$ compounds (peaks 5–8). A SIC plot of *m/e* 252, 356, 358, and 360 ions shows that the next six peaks, excluding *o,p'*-BA (peak 11), are isomers of peak 9 with similar structures (Figure 14). A total of eight isomers of structure **13** could be formed, and seven peaks having this MS fragmentation pattern are observed (peaks 9–16, excluding peak 11). Another isomer peak may coelute with the larger *o,p'*-BA, which would account for each of the possible isomers of **13** in the chromatograph. As **13** is most likely formed from a cycloaddition reaction of BCB and a stilbene compound,

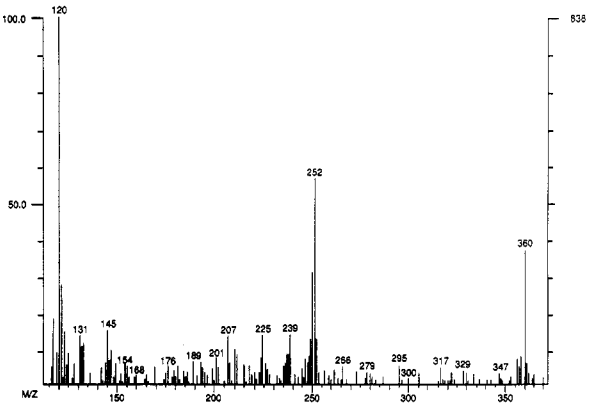


**Figure 13.** MS of peak 9 in LC of cross-linked BCB PC hydrolysate.

**Scheme 6. MS Fragmentation of BCB-OH Trimer 12**

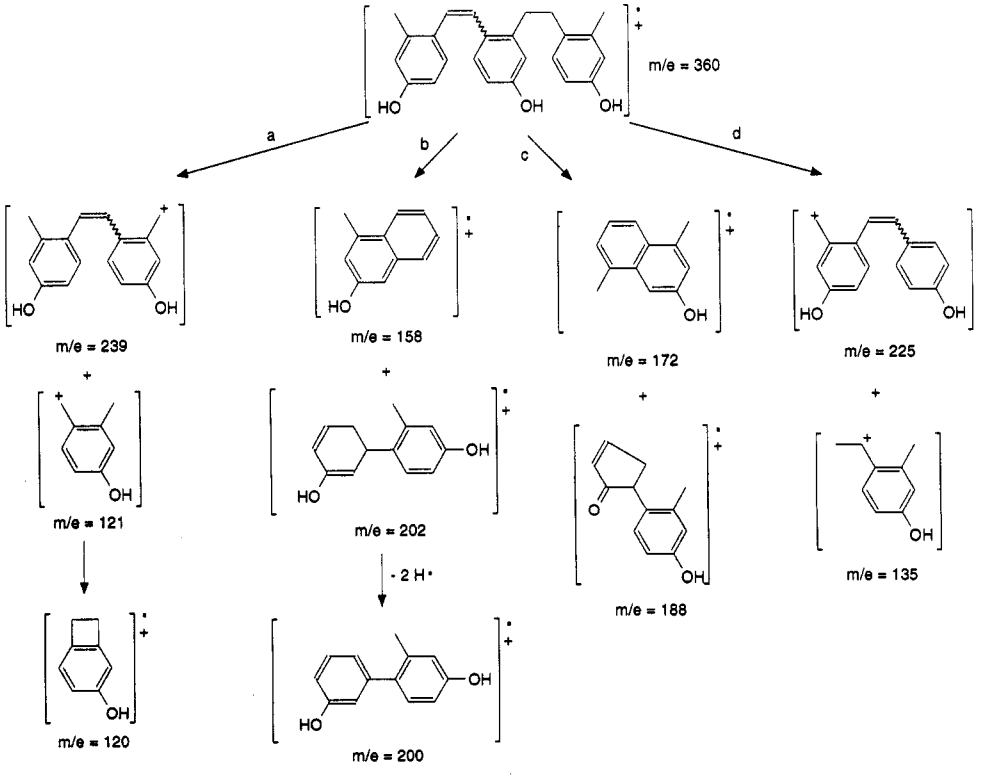

**Scheme 7. MS Fragmentation of BCB-OH Trimer 13**

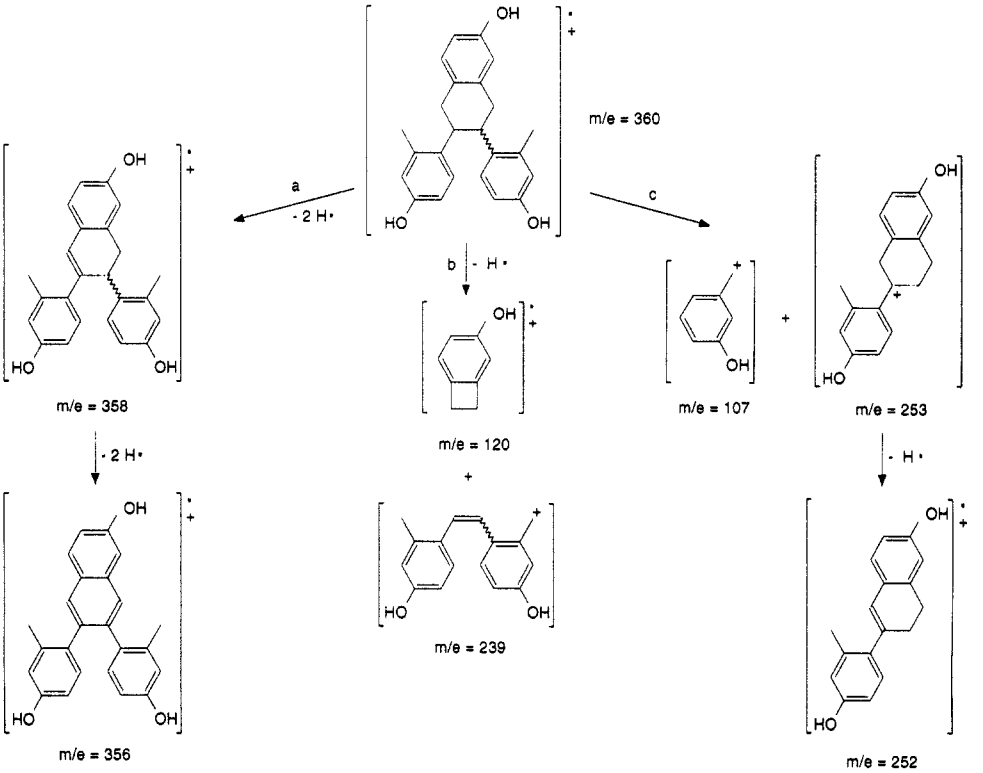


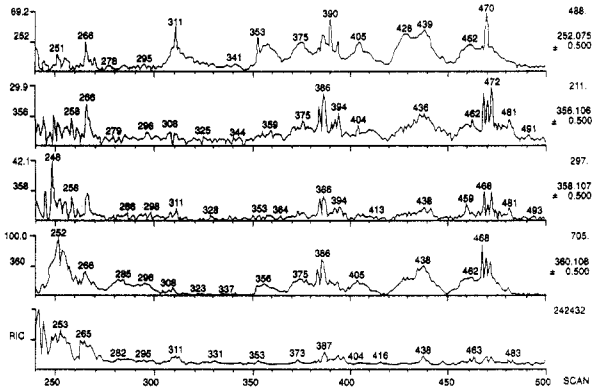

**Figure 14.** SIC's of *m/e* 252, 356, 358, and 360 in LC of cross-linked BCB PC hydrolysate.

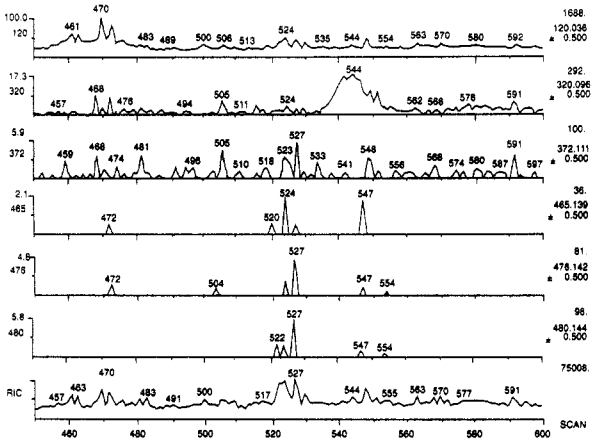

**Figure 15.** SIC's of *m/e* 120, 320, 372, 465, 476, and 480 in LC of cross-linked BCB PC hydrolysate.

its presence argues strongly for a stilbenic structure for peaks 2 and/or 3.

Mass spectra of peaks 17–19 could not be obtained from this sample due to their low concentration, but a SIC plot of *m/e* 480, 476, 465, and 372 ions indicate that these last peaks have $M^+$ of *m/e* 480 and are isomers of tetrahydronaphthalene compound **14** (Figure 15). The M-4 ion gives aromatization of the unsaturated ring, the M-15 ion arises from methyl fragmentation, and the M-108 ion results from loss of a hydroxytolyl radical (Schemes 9–12 described below). These components are not considered to be homologs of compound **13** because such isomers would not produce M-2 and M-4 ions.

**Synthesis, Cross-Linking, and LC/MS Analysis of Bis-BCB $CO_3$.** Bis-BCB $CO_3$ (**15**) was prepared from BCB-OH (**2**) and phosgene under interfacial conditions (Scheme 8). Bis-BCB $CO_3$ samples were degassed and sealed in glass tubes under $N_2$ and then cross-linked by heating at 200 °C for 30 min, increasing the temperature to 300 °C at 1 °C/min, and then heating at 300 °C for 1 *h*. The cross-linked product was hydrolyzed in THF/KOH/methanol, acidified with 1 N HCl, and extracted into diethyl ether. Evaporation gave the mixture of phenolic poly-BCB compounds as a brown, friable solid.

**Scheme 8. Synthesis of Bis-BCB $CO_3$ (15)**

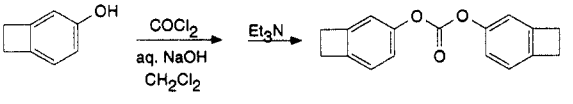


**2** **9**

LC analysis of cross-linked bis-BCB $CO_3$ hydrolysate shows, using the LC/MS results from BCB PC hydrolysate as a guide, a considerable amount of unreacted BCB-OH (**2**; peak 1), the previously observed BCB-OH dimers **9** or **10** (peaks 2 and 3, respectively), a new peak (4) at about 27 min which in earlier analyses was masked by *p,p'*-BA, the previously observed BCB-OH trimers **12** at about 27–29 min (peaks 5–8), and a complex mixture of compounds at 30–40 min (Figure 16). (The retention times in this analysis are offset from the earlier one due to the use of a new LC column.) The resolution in this chromatograph is somewhat poorer than that obtained in the analysis of BCB PC hydrolysates, particularly in the regions of the BCB-OH trimers and tetramers. At least part of the complexity of the latter part of this chromatograph can be attributed to side reactions of the poly-BCB products

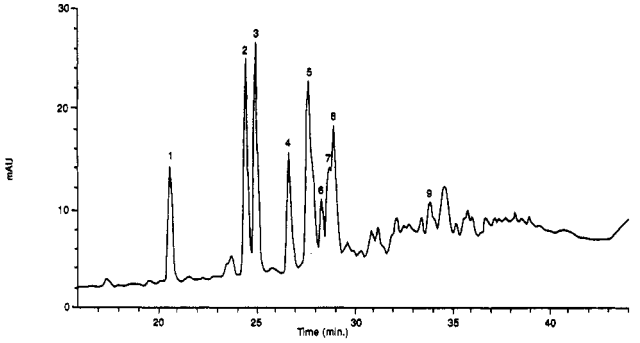


**Figure 16.** LC of cross-linked Bis-BCB $CO_3$ hydrolysate.

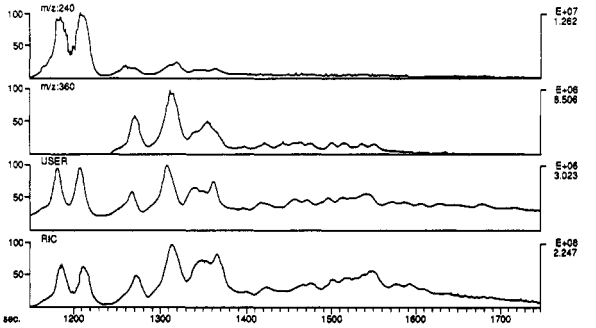


**Figure 17.** SIC's of *m/e* 240 and 360 in LC of cross-linked bis-BCB $CO_3$ hydrolysate.

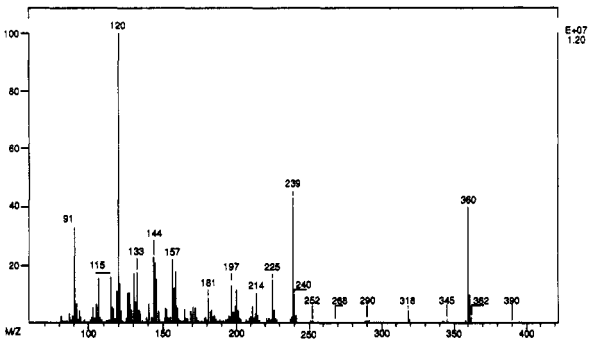


**Figure 18.** MS of peak 4 in LC of cross-linked bis-BCB $CO_3$ hydrolysate.

either during cross-linking, during hydrolysis, or both. BCB-OH trimers **13** and tetramers **14** contain several benzylic hydrogen atoms and are expected to be prone to oxidative side reactions, and oxygen was not rigourously excluded from the samples. The relative area percent of the first eight peaks appears in Table 2.

LC/MS analysis of cross-linked bis-BCB $CO_3$ hydrolysate provides MS data analogous to that found for BCB PC hydrolysate described above. Plots of the reconstructed ion chromatograph (RIC), the LC UV detector response (USER), and *m/e* 240 and 360 selected ion chromatographs (SIC) show that the most intense responses are due to BCB-OH dimers and trimers (Figure 17). Spectra of the first two peaks show molecular ions ($M^+$) at *m/e* 240 and a fragmentation pattern essentially identical to the corresponding peaks in BCB PC hydrolysate.

MS of peak 4 shows it to be another isomer of BCB-OH trimer **12** by virtue of its $M^+$ at *m/e* 360 and fragmentation pattern, which is essentially the same as that found in BCB PC hydrolysate (Figure 18). With the additional isomer of **12** found, a total of 5 of the 16 possible isomers are observed in this LC method. Peaks 5–8 show $M^+$ at *m/e* 360 and ion fragments as described above the BCB-OH trimer **12**.

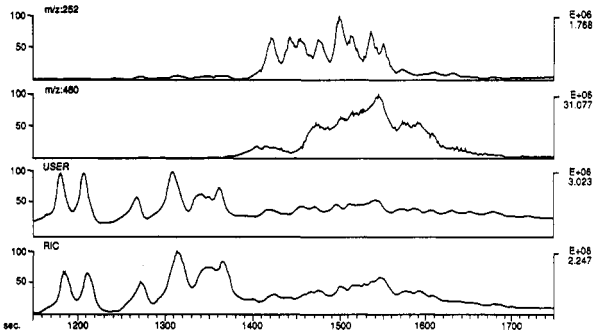


**Figure 19.** SIC's of *m/e* 252 and 480 in LC of cross-linked bis-BCB $CO_3$ hydrolysate.

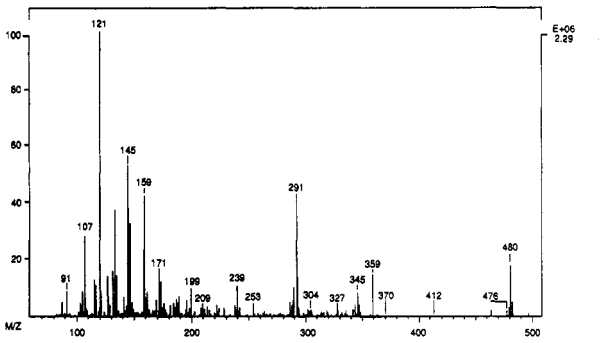


**Figure 20.** MS of peak 9 in LC of cross-linked bis-BCB $CO_3$ hydrolysate.

The latter portion of the chromatograph is also poorly resolved in the LC/MS analysis. SIC's of *m/e* 480 and 252 (a major fragment of BCB-OH trimer **13**) show that many of the compounds eluting in this region are BCB-OH trimers and tetramers (Figure 19). Unlike the previous study, this sample contains a large enough concentration of BCB-OH tetramers to obtain a mass spectrum (peak 9, Figure 20). The BCB-OH tetramer fragments observed are consistent with the previously reported SIC's and structural assignment to **14**. Fragmentation of BCB-OH tetramer **14** follows several paths, many of which are analogous to the lower molecular weight analogs: (a) dehydrogenation in two successive steps to form the dihydronaphthalene and the naphthalene derivatives (Scheme 9); (b) homolysis of the disubstituted ethane carbon–carbon bond to a bis(hydroxytolyl)tetrahydronaphthalenic ion and dimethylphenol ion (Scheme 9); (c) similar *m/e* fragments as in path b by retro-Diels–Alder reaction to a dehydrotrihydroxytris(*o*-xylene) ion and BCB-OH ion (Scheme 10); (d) homolysis of the phenylcyclohexane carbon–carbon bond to a hydroxytolyl ion and a [[(hydroxymethylphenyl)ethyl]hydroxyphenyl]-tetrahydronaphthalenic ion, which subsequently fragments by phenyl ring cleavage to a 1-(hydroxyphenyl)-2-(hydroxytolyl)ethane ion and a hydroxydihydronaphthalene, which then loses a hydrogen atom to give the indicated ion (Scheme 10); (e) an unsymmetrical cleavage of the hydroxyphenyl ring to form dihydroxymethylbiphenol, which subsequently loses formaldehyde and hydrogen atoms, and a tetrahydrophenanthrene derivative, which then undergoes a retro-Diels–Alder reaction to yield a hydroxymethylnaphthalene ion (Scheme 11); and (f) a symmetrical cleavage of the hydroxyphenyl ring to form another tetrahydrophenanthrene derivative, which then yields a dimethylhydroxynaphthalene ion, and a (oxocyclopentenyl)hydroxytolyl ion, which can lose hydrogen atoms and carbon monoxide to form various cyclopentadienyl derivatives (Scheme 12). These reasonable fragmentation pathways account for all of the major fragments observed, are consistent with the fragmentation

**Scheme 9. MS Fragmentation of BCB-OH Tetramer 14**

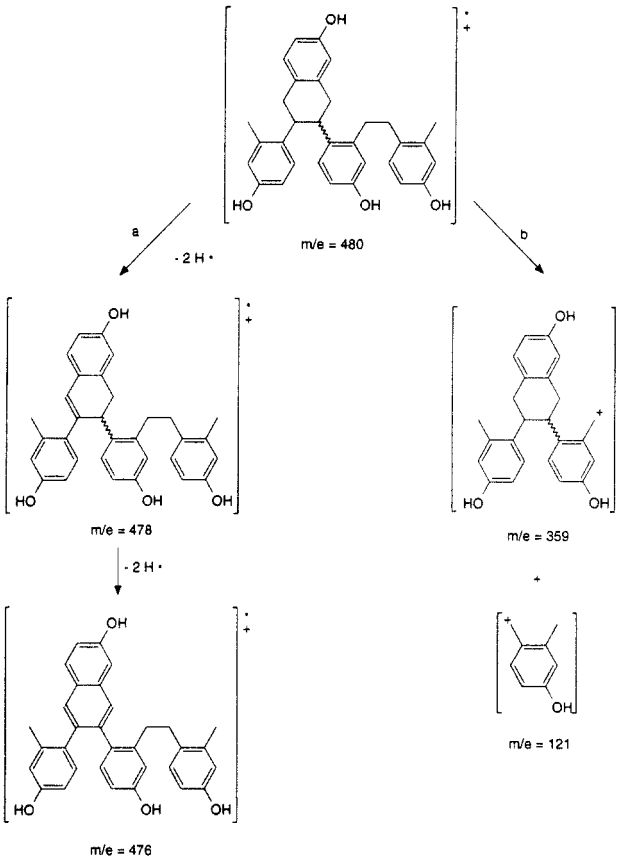


routes proposed with the lower molecular weight homologs, and thus support the structural assignment to BCB-OH tetramer **14**.

The distribution of the poly-BCB products observed allows estimation of the network functionality. Since the response factors for these products are not currently known, the relative concentration of each component cannot be rigorously quantified. But, assuming that each component has the same response factor, integration of the poly-BCB product peaks in the LC's gives an average functionality of the poly-BCB products of about 2.6. Also, it should be emphasized that these LC/MS analyses of the BCB PC and bis-BCB $CO_3$ cross-link junction products provide revealing, yet general, structural information about these compounds. Important details about these structures, in particular the regio- and stereochemistry of the various isomers, require analysis by other techniques.

**Reaction Mechanisms.** The formation of all of the BCB homopolymerization products observed in the cross-linking of BCB PC and bis-BCB $CO_3$ can be rationalized by Diels–Alder cycloadditions and free-radical reactions, although several other expected free radical derived products are not observed. Dibenzocyclooctane **10** can form from homolysis and diradical coupling as shown in Scheme 1. Two 1,5 hydrogen atom shifts in the same dimer diradical (**16**) can yield stilbene **9**, and a Diels–Alder cycloaddition of it and the *o*-quinodimethane intermediate (**17**) would give trimer **13** (Scheme 13, where R = PC in the polymer or –OH in the hydrolysate). Trimer **12** could arise from addition of the diradical **16** to the *o*-quinodimethane **17** and subsequent hydrogen atom shifts, and tetramer **14** would follow from another Diels–Alder cycloaddition with the *o*-quinodimethane **17** (Scheme 14).

However, several likely BCB homopolymerization products arising from diradical **16** are not observed. Diradical **16** and its homologs should readily form indanes, such as **18**, by a [1,5] H shift and subsequent diradical coupling.

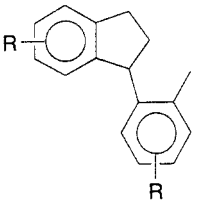

**18**

Indanes have distinctive MS fragmentation paths,[21] so it

**Scheme 10. MS Fragmentation of BCB-OH Tetramer 14**

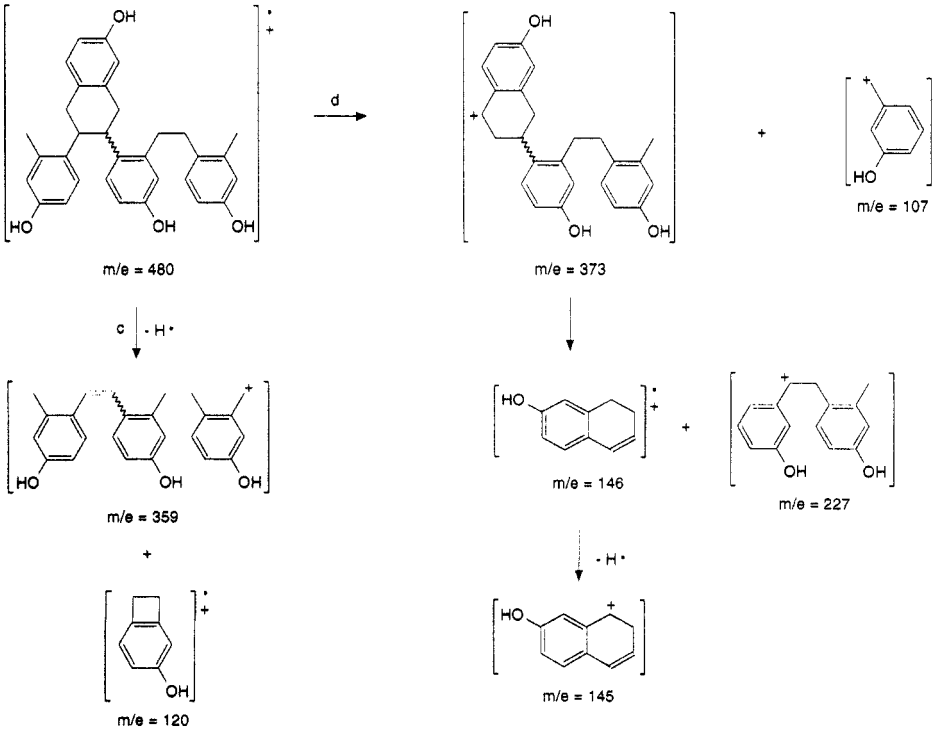

**Scheme 11. MS Fragmentation of BCB-OH Tetramer 14**

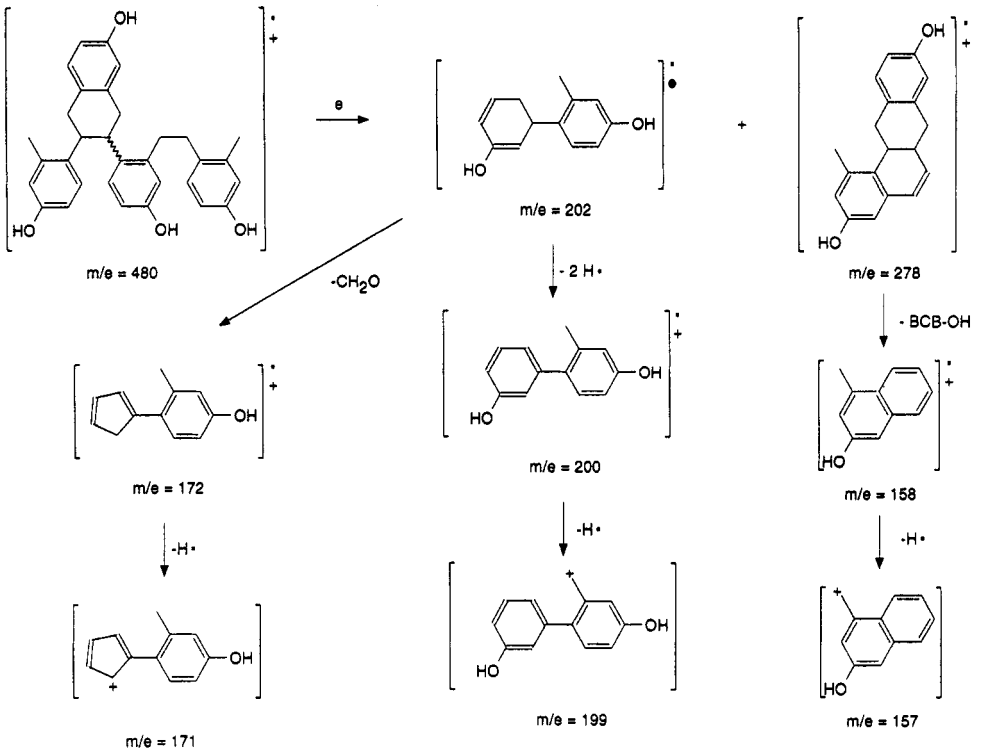


**Scheme 12. MS Fragmentation of BCB-OH Tetramer 14**

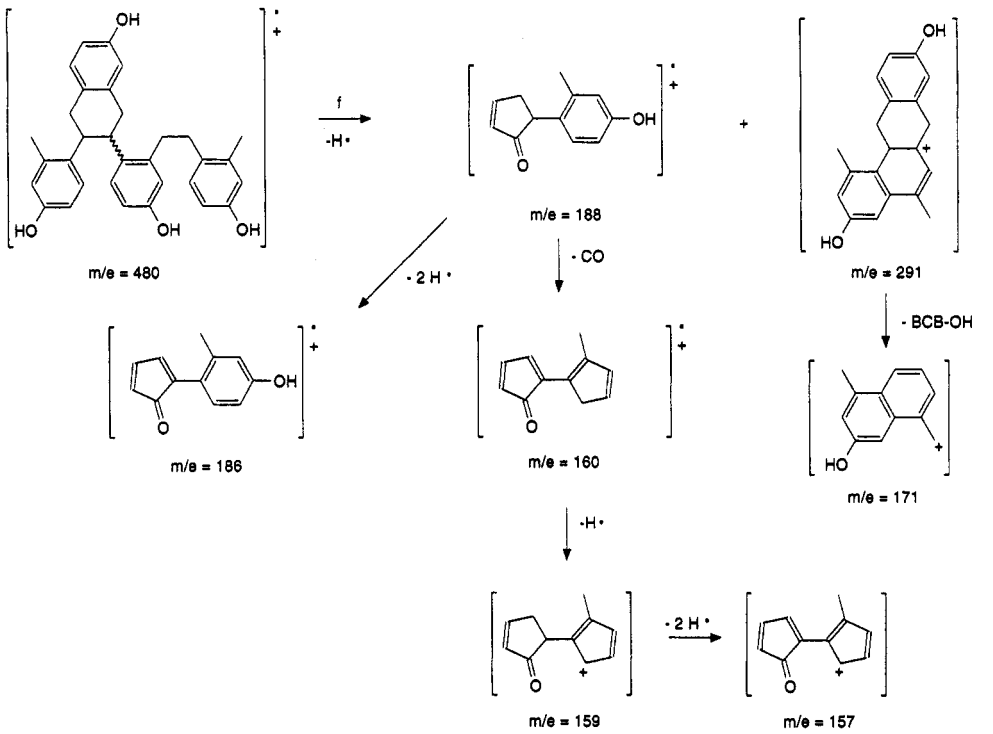


**Scheme 13. Radical Mechanism to BCB-OH Dimer 9**

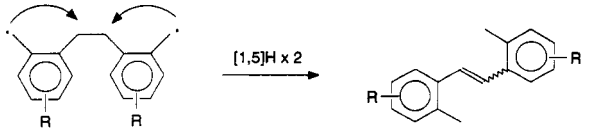


16 9

is clear that such compounds are absent in the products. Another group of absent compounds would result from coupling of diradical **16** to tetramer **19** and homologs through poly(*o*-xylene). In addition to these coupling reactions, two types of radical chain-transfer reactions are expected from diradical **16**. The benzylic hydrogens in trimers **12** and **13** and tetramer **14** would readily transfer to diradical **16** to form the disproportionated products. Also, radicals such as **16** would abstract hydrogen atoms from the BA PC chain and thereby initiate its degradation.[22] In fact, no evidence of BA PC degradation products, particularly isopropenylphenol and its oligomers, is observed in the BCB PC and bis-BCB $CO_3$ hydrolysates. Thus, considering all of the likely radical reaction products which are not observed, it is deemed unlikely that radical intermediates are involved in the cross-linking of BCB PC and bis-BCB $CO_3$.

**Scheme 14. Radical Mechanism to BCB-OH Trimer 12**

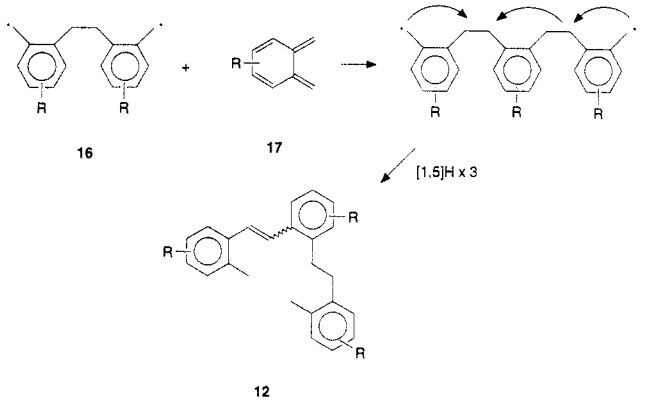

The mechanism of the thermal cross-linking of BCB PC and bis-BCB $CO_3$ must account for several observations: cross-linking only involves reactions of BCB moieties, only poly-BCB products having from two to four BCB units are formed, unreacted BCB-OH remains in the networks, and expected reaction products from radical intermediates are not evident. A reaction mechanism which can account for these observations involves Diels–Alder cycloadditions, retro-ene reactions, and sigmatropic rearrangements.

The first reaction in such a BCB homopolymerization mechanism is the cycloaddition reaction of two *o*-quinodimethanes **17** (R = PC or –OH in hydrolysate) to form BCB spirodimer **11**, as previously shown[11,23] (Scheme 15). Two types of rearrangements of **11** which lead to observed BCB products are depicted using projections **11a** and **11b**. In these projections the benzocyclohexane ring is shown in half-chair conformations with the spirocyclohexadiene ring in a pseudoequatorial position in **11a** and in a pseudoaxial position in **11b**. A thermally allowed [1,3] suprafacial sigmatropic rearrangement of **11a** proceeds with inversion of the configuration of benzocyclohexane C-1 to form dibenzocyclooctadiene **10**. The geometry of **11a** is appropriate for this rearrangement, with models indicating a C-1 to C-3 distance of about 2.8 Å. An analogous [1,3] rearrangement of substituted bicyclo[1.1.2]-hex-2-enes **23** occurs at 150–200 °C with activation enthalpies of 25–35 kcal/mol to give exo isomer **24**.[24]

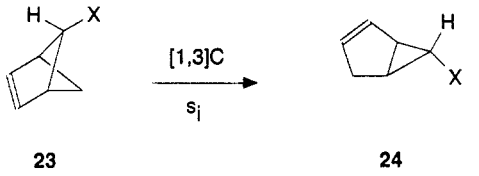

Models show that the distance between bridgehead C-1 and C-3 is about 2.1 Å; thus the 2.8-Å distance involved in the rearrangement of **11a** is quite reasonable.

In spirodimer conformation **11b** the exocyclic methylene group of the pseudoaxial cyclohexadiene points directly at the axial hydrogen on the opposite benzylic carbon. Models of **11b** show both a reasonable geometry and appropriate through-space C–H distance (about 2.0 Å) for a [1,7] retro-ene reaction to **20** (Scheme 15). While the great majority of known retro-ene reactions are six-electron, [1,5] rearrangements,[25] the eight-electron, [1,7] retro-ene rearrangement of homoallyl ethers **25** and **26** was shown.[26] The driving force for rearrangement of **11b**

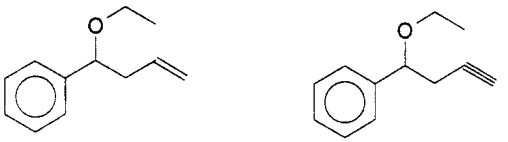

is the relief of ring strain and the eventual aromatization of the second ring by a [1,5] H sigmatropic rearrangement of **20** to **9**. The geometry of **20a** as formed from the retro-ene reaction would yield upon [1,5] H rearrangement the *cis* isomer of **9**, and this stereochemistry is indicated by its UV spectrum (absorbance maximum = 280 nm in THF; Figure 8). This very type of sigmatropic rearrangement has been observed in dibenzocyclooctadiene derivative **28**, formed by $SO_2$ extrusion of the disulfoxide of **27**, to form dibenzocyclooctadiene **29** (Scheme 16).[27]

An interesting example illustrating the importance of geometry in the outcome of pericyclic rearrangements arises in the thermolysis of dipropenylbenzenes **30** and **32**

**Scheme 15. Pericyclic Reaction Mechanism for BCB PC Homopolymerization**

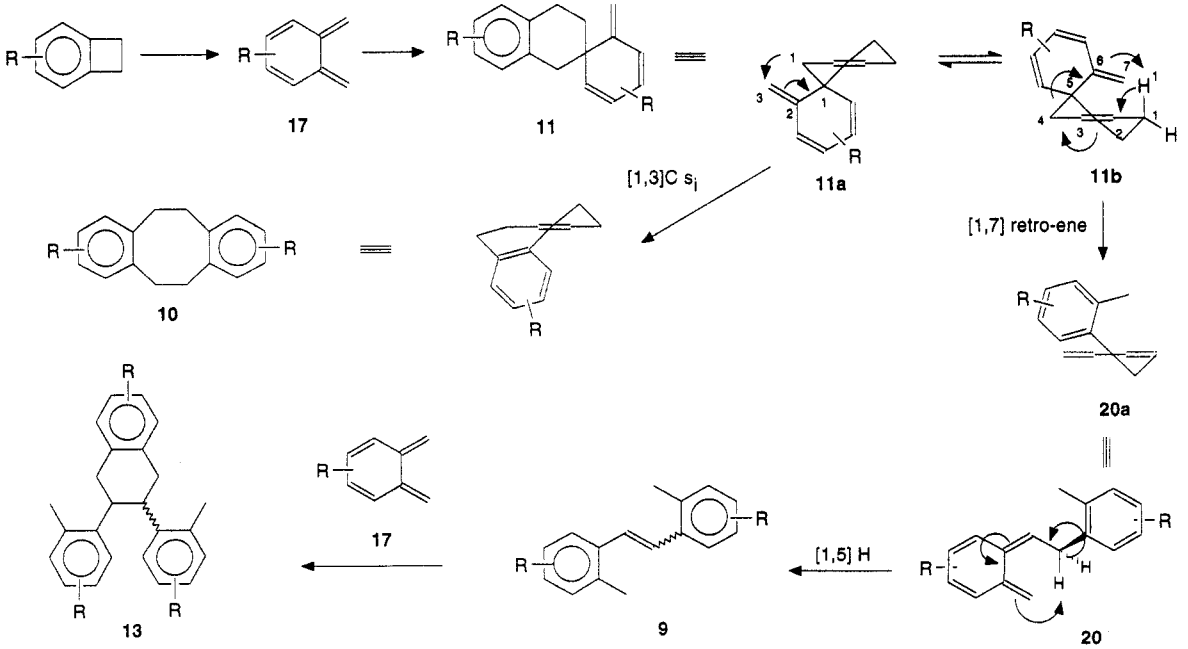

**Scheme 16. [1,5] H Sigmatropic Rearrangement of Polyene 28**

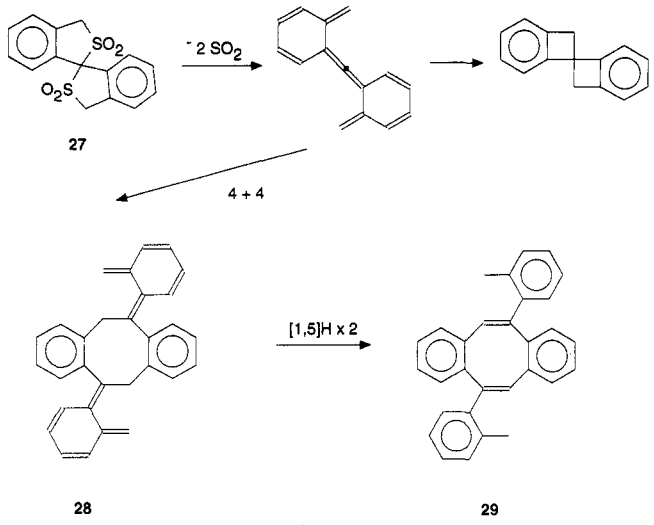


**Scheme 17. Thermolysis of Dipropenylbenzenes 30 and 32**

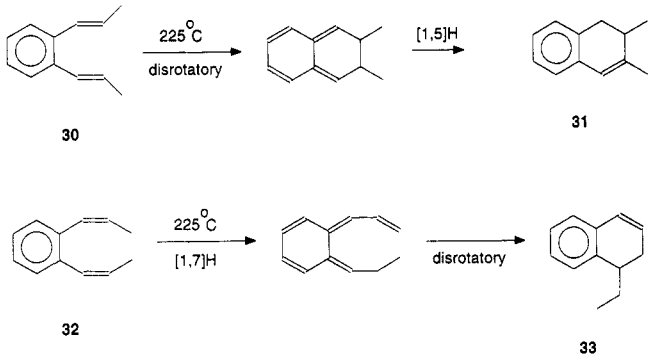


(Scheme 17).[28] The *trans* isomer undergoes a Cope rearrangement followed by a [1,5] H shift to form dihydronaphthalene **31**, whereas due to a favorable geometry the *cis* isomer first undergoes an antarafacial [1,7] H sigmatropic rearrangement and then the Cope rearrangement to **33**. Antarafacial [1,7] sigmatropic rearrangements require a twisted conformation to comply with conservation of orbital symmetry rules,[29] and this geometry is produced by the *cis* configuration in **32** and by the spiro junction in **11**. As in the radical mechanism described above, tetrahydronaphthalene **13** is likely formed by the Diels–Alder cycloaddition of *o*-quinodimethane **17** and stilbene **9** (Scheme 15).

Spirodimer **11** contains an exocyclic carbon–carbon double bond which can participate in another Diels–Alder cycloaddition reaction with *o*-quinodimethane **17** to yield "spirotrimer" **21** (Scheme 18). Spirotrimer **21** can exist in two conformers **21a** and **21b**, with **21a** the favored one by virtue of its bulky ring system in a pseudoequatorial position. In minor conformation **21b**, with the ring system in a pseudoaxial position, C-9 is about 2.1 Å from the opposite benzylic axial hydrogen which is well within range of the depicted [1,9] retro-ene rearrangement to **22**. The second spiro junction in **21b** provides the required double-twisted geometry for this suprafacial rearrangement. No precedent for this type of retro-ene reaction was found in the literature, and even [1,9] sigmatropic rearrangements are rare. One system proven to undergo thermal [1,9] suprafacial sigmatropic rearrangements is the substituted tropone **34**.[30]

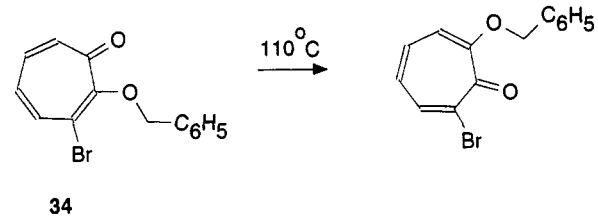


From polyene **22** to dehydrotris(*o*-xylene) **12** requires only facile [1,5] and [1,3] H sigmatropic shifts (Scheme 18). The [1,5] H rearrangement was discussed above, and [1,3] H shifts in toluene isomers are well-known.[31] Although this [1,3] H rearrangement cannot be concerted according to orbital symmetry rules, the diradical transition state involved, as seen in isotoluene isomerizations,

**Scheme 18. Pericyclic Reaction Mechanism for BCB PC Homopolymerization**

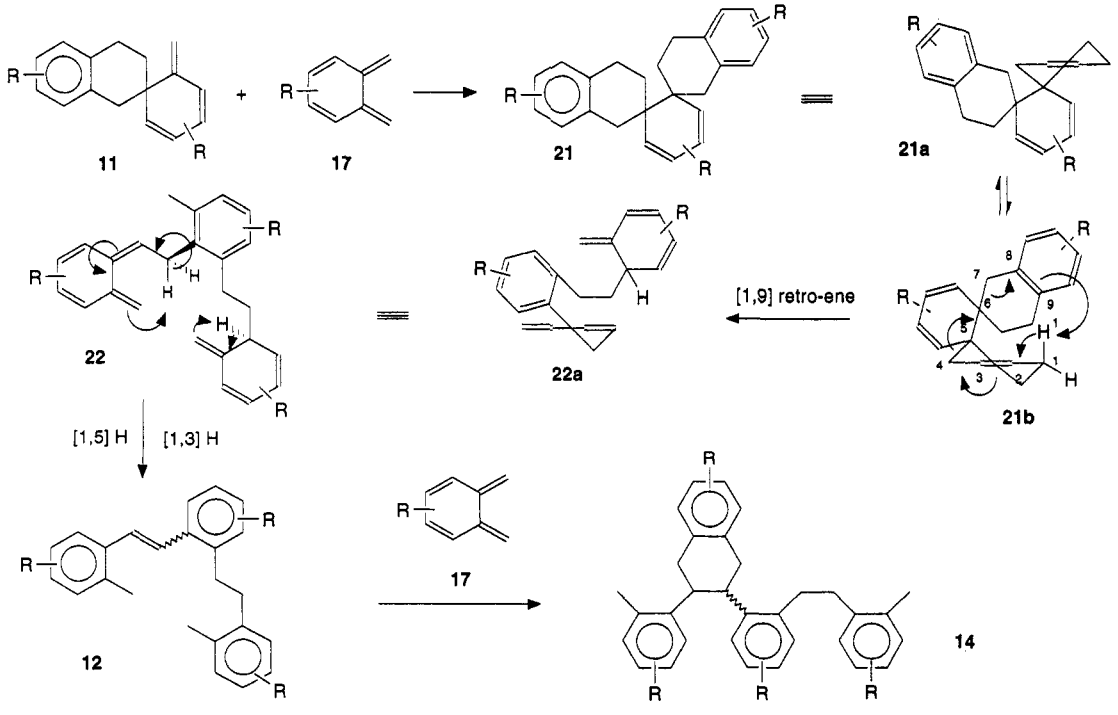

should not lead to radical side reactions.

The highest molecular weight poly-BCB product observed can be accounted for by another Diels–Alder cycloaddition of *o*-quinodimethane **17** to dehydrotris(*o*-xylene) **12** to yield tetramer **14** (Scheme 18). By this pericyclic mechanism, no higher molecular weight poly-BCB products can be formed since neither spirotrimer **21** nor tetrahydronaphthalene **14** can react further with *o*-quinodimethane **17**.

## Conclusions

LC/MS analyses of the hydrolysates of cross-linked BCB PC and cross-linked bis-BCB $CO_3$ show that the cross-linking products result solely from BCB homopolymerization and consist of, in addition to unreacted BCB-OH (**2**), BCB dimers, trimers, and tetramers. The data support the identification of these BCB oligomers as hydroxy-substituted stilbenes and/or dibenzocyclooctadienes (which cannot be distinguished by MS analysis) and hydroxy-substituted tetrahydronaphthalenes. The primary BCB reaction products were found to be the difunctional dihydroxydimethylstilbenes **9** and/or dihydroxydibenzocyclooctadiene **10** and the trifunctional dehydrotris(hydroxyxylene) (**12**). Lesser concentrations of trifunctional 2,3-bis(hydroxytolyl)hydroxy-1,2,3,4-tetrahydronaphthalene (**13**) and tetrafunctional tetrahydronaphthalene **14** were also identified. These compounds can have several regio- and stereoisomers, each of which either are not produced in the cross-linking reaction or, more likely, are not resolved by the chromatography. Further analytical studies are required to ascertain the regio- and stereochemistry of these compounds.

The presence of BCB-OH in the hydrolysates shows conclusively that the intermediate *o*-quinodimethane **17** does not react with BA or carbonate segments in BA PC. The absence of 3,4-dimethylphenol, the product formed from hydrogen abstraction of a ring-opened BCB, was confirmed. The persistance of BCB groups in the cross-linked network results from trapping of unreacted polymer chain ends after gelation; apparently BCB end groups which lack mobility to encounter reactive olefins during cross-linking remain in the mixture unreacted. Based on the approximate relative concentrations of the poly-BCB-OH products observed, the average network functionality of BCB PC and bis-BCB $CO_3$ is estimated to be about 2.6.

A previously proposed diradical mechanism which could account for the observed BCB homopolymerization products is not consistent with the selectivity of these products. Only certain BCB dimers, trimers, and tetramers are observed, several diradical reaction products expected from such intermediates are not found, and products derived from BA PC chain-transfer and radical addition reactions do not appear. Therefore, a diradical reaction mechanism of BCB PC thermal cross-linking is considered unlikely.

The formation of the observed BCB homopolymerization products identified in thermally cross-linked BCB PC's can be fully explained by a series of pericyclic reactions. This proposed mechanism involves Diels–Alder cycloadditions, a suprafacial [1,3] carbon–carbon sigmatropic rearrangement, an antarafacial [1,7] retro-ene reaction, a suprafacial [1,9] retro-ene reaction, suprafacial [1,5] hydrogen sigmatropic rearrangements, and a [1,3] hydrogen shift. Each of the sigmatropic rearrangements and retro-ene reactions are thermally allowed processes. This mechanism fully accounts for the types and range of products observed in cross-linked BCB PC's and explains why additional products are not formed.

Precedents for the [1,3] suprafacial sigmatropic rearrangement and the [1,7] retro-ene reaction are known. The suggested [1,9] retro-ene reaction may be unprecedented, but the intermediate involved has both a very unusual geometry and the required suprafacial orbital overlap and appropriate carbon–hydrogen distance to undergo this reaction.

**Acknowledgment.** The authors thank Dr. L. A. Shadoff, Dr. N. Rondan, and Prof. E. Huyser (University of Kansas) for helpful discussions.

## References and Notes

(1) Marks, M. J.; Sekinger, J. K. *Macromolecules* **1994**, *27*, 4106.
(2) Marks, M. J.; Schrock, A. K.; Newman, T. H. U.S. Patent 5, 171,824, Dec 18, 1992.
(3) Marks, M. J.; Schrock, A. K.; Newman, T. H. U.S. Patent 5, 198,527, Mar 30, 1993.
(4) Partridge, I. K. In *Advanced Composites*; Partridge, I. K., Ed.; Elsevier: New York, 1989; p 7.
(5) Kirchhoff, R. A.; Bruza, K. J. *Chemtech* **1993**, *Sept*, 22.
(6) Kirchhoff, R. A.; Carriere, C. J.; Bruza, K. J.; Rondan, N. G.; Sammler, R. C. *J. Macromol. Sci., Chem.* **1991**, *A28* (11 & 12), 1079.
(7) Iwatsuki, S. *Adv. Polym. Sci.* **1984**, *85*, 93.
(8) Tan, T. S.; Arnold, F. E. *J. Polym. Sci., Polym. Chem. Ed.* **1988**, *26*, 1819.
(9) Klundt, I. L. *Chem. Rev.* **1970**, *70*, 471.
(10) Oppolzer, W. *Synthesis* **1978**, 793.
(11) Charlton, J.; Alauddin, M. *Tetrahedron* **1987**, *43*, 2873.
(12) Hahn, S. F.; Martin, S. J.; McKelvy, M. L. *Macromolecules* **1992**, *25*, 1539.
(13) Hahn, S. F.; Martin, S. J.; McKelvy, M. L.; Patrick, D. W. *Macromolecules* **1993**, *26*, 3870.
(14) ASTM uncertified mass spectrum no. 31336.
(15) ASTM uncertified mass spectrum no. 31334.
(16) Mintas, M.; Jakopcic, K.; Klasinc, L.; Gusten, H. *Org. Mass Spectrom.* **1977**, *12*, 544.
(17) Sample prepared by K. J. Bruza, MS obtained by D. W. Patrick, both of Dow Central Research, unpublished results.
(18) Bowie, J.; White, P. *Org. Mass Spectrom.* **1972**, *6*, 135.
(19) Ito, Y.; Nakatsuka, M.; Saegusa, T. *J. Am. Chem. Soc.* **1982**, *104*, 7609.
(20) Mass Spectral Data, American Petroleum Institute Research Project 44, Texas A&M University, serial no. 201-m, Oct 31, 1968.
(21) Arnold, D. R.; Fahie, B. J.; Lamont, L. J.; Wierzchowski, J.; Young, K. M. *Can. J. Chem.* **1987**, *65*, 2734.
(22) Carlsson, D. J.; Wiles, D. M. Degradation. *Encyclopedia of Polymer Science and Technology*; Wiley: New York, 1987; Vol. 4, p 630.
(23) Errede, L. A. *J. Am. Chem. Soc.* **1961**, *83*, 949.
(24) Roth, W.; Friedrich, A. *Tetrahedron Lett.* **1969**, 2607.
(25) Desimoni, G.; Tacconi, G.; Barco, A.; Polline, G. *Natural Products Synthesis Through Pericyclic Reactions*; ACS Monograph Series 180; American Chemical Society: Washington, DC, 1983; pp 354–358.
(26) Viola, A.; Madhavan, S.; Proverb, R. J.; Yates, B. L.; Larrahondo, J. *J. Chem. Soc., Chem. Commun.* **1974**, 842.
(27) Cava, M.; Kuczkowski, J. *J. Am. Chem. Soc.* **1970**, *92*, 5800.
(28) von Heimgartner, H.; Hansen, H.; Schmid, H. *Helv. Chim. Acta* **1970**, *53*, 173.
(29) Woodward, R. B.; Hoffmann, R. *The Convervation of Orbital Symmetry*; Springer-Verlag: Weinheim, Germany, 1970.
(30) Sugiyama, S.; Mori, A.; Takeshita, H. *Chem. Lett.* **1987**, 1247.
(31) Bailey, W. J.; Baylouny, R. A. *J. Org. Chem.* **1962**, *27*, 3476.
(32) Thomas, P. J.; DeVries, R. A., Pews, R. G.; Batzel, D. A. U.S. Patent 5,227,536, Jul 13, 1993.